A Contextual Sensor System for Non-Intrusive Machine Status and Energy Monitoring

Yutian Ren^{a,b}, Guann-Pyng Li^{a,b,*}

ARTICLE INFO

Keywords: Smart Manufacturing Cyber Physical Systems Industrial IoT Worker Machine Interaction Energy Disaggregation Context Awareness

ABSTRACT

Event-driven contexts in manufacturing occur pervasively as a result of interactions among involved entities such as machines, workers, materials, and environment. One of the primary tasks in smart manufacturing is to derive a context-aware system conveniently incorporating worker knowledge for generating timely actionable intelligence for workers on factory floor and supervisors to respond. In this paper, we propose to design a human-and-machine interaction recognition framework by using a causality concept to collect contextual data for classifications of normal and abnormal machine operations. The causes and effects are between workers and machines for this initial research. To apply the causality to recognize worker interactions, initially a reliable way to identify the states of machines is necessary. The proposed contextual sensor system, consisting of a power meter for measuring machine operation conditions, a visual camera for capturing worker and machine interactions via a finite state machine model, and an algorithm for determining power signatures of individual components via energy disaggregation is implemented on semiconductor fabrication machines (manual or PLC controlled) each with multiple components. The experiment results demonstrate its context extraction capability such as components states and their corresponding energy usage in real time as well as its ability to identify anomalous operation conditions.

1. Introduction

In smart manufacturing (SM), cyber physical systems (CPS) call for the enhancement of context-awareness of manufacturing machines and factory operations by contextualizing the sensed signals, detected events, and recognized surroundings so that it is capable of providing actionable intelligence to improve operational integrity, energy productivity, and machine prognostics and health management (PHM) [1, 2]. To transform the data into actionable intelligence, two popular frameworks have been proposed and conceptually implemented. One is to leverage the data generated in current manufacturing systems and transfer them to computing services for contextual machine learning (ML) [3, 4]. Another is to design a context-aware system with manufacturing engineers by incorporating additional IoT sensors into available information from manufacturing execution systems for ML [5, 6]. However, both frameworks have not leveraged the contextual sensing capability of workers in real time on factory floors to complement the data generated by IoT sensors and existing manufacturing systems. Thus, an alternative contextual system design capable of incorporating the intelligence of shop floor workers, i.e., human senses and knowledge/experience, in real time is worthwhile exploring.

While systems allowing workers on the floor to input information via computers have been developed, they have not been successfully integrated into existing manufacturing systems due to natural language inputs not compatible with

Email addresses: yutianr@uci.edu (Y. Ren); gpli@calit2.uci.edu (G.

ORCID(s):

Li)

data from machines. Additionally, workers are required to proactively input readable information, but it is not well accepted by workers due to sociological reasons according to a questionnaire [7]. These barriers motivate us to search an alternative way of connecting workers. In fact, workers are naturally connected to manufacturing systems through their active and reactive interactions with machines [8]. Workers' active and reactive interactions contain meaningful context values in the form of causes and effects. For example, workers as causes by following standard operation procedures (SOP) actively operate machines and machines change states as effects. On the other hand, machines behaving abnormally as causes result in workers reactively responding to machine operation conditions. By understanding worker interactions in the active and reactive aspects, the contextual information regarding regular operation and anomalies can be extracted.

To understand the worker machine interactions (WMI), a methodology to reliably to capture and confirm workers' intended inputs via gesture recognition is proposed in this work for capturing the time and location of happenings on the floor, which can commensurate real time data from existing manufacturing systems. The interaction data captured on the floor can then be used in ML for developing classifications of manufacturing conditions such as normal operation, operator errors, and machine warnings. This set of manufacturing classifications can further support an existing manufacturing system in dynamically adjusting its execution commands for the machine fault prevention, workflow optimization, and energy productivity improvement.

The development of the WMI recognition system is based on the concept of well-established causality between workers and machines rather than supervised ML routines of manual data labeling and model training. A causally correlated Finite

^aDepartment of Electrical Engineering and Computer Science, University of California, Irvine, CA 92697, USA

^bCalifornia Institute for Telecommunications and Information Technology (Calit2), University of California, Irvine, CA 92697, USA

^{*}Corresponding author

State Machine (FSM) model is established in this study to model the timing and causal behaviors of machines and workers during manufacturing processes. The design of FSM can leverage not only existing knowledge and experience from workers but also documented standard operating procedures (SOP) and machine operation manuals to extract the known causes and effects. The WMI recognition developed from FSM at normal operation conditions offers a class of various human gestures representing the contextual information of active healthy interactions. The anomaly detection of floor operation can then be determined when the worker reactive gestures fall out of the norms or the machine operates out of its functional states.

Conventionally, the reliable understanding of WMI requires advanced ML models with well-labeled dataset for training [9]. With the causality between workers and machines identified, the confirmation from the machine side as causes or effects provides an adaptive way of capturing WMI contexts as training data. Thus, initially a reliable method of observing machine states to automatically capture the data of causally related worker interactions becomes more applicable as the first step. The captured WMI contexts can then be used for the ML training of WMI recognition. For situation awareness of machine operation in the causeand-effect method, machine states with their corresponding observable quantified contents are needed. For example, power signatures of individual components at states of active, idle, and off in each machine can be measured and presented as a cause of deviation from norms for workers to react.

To illustrate the concept of the causality-inspired contextual WMI recognition system, as the first step, this paper builds a contextual sensor system with a security video camera for capturing WMI contexts in identifying causes of interaction and a power meter for observing the effects of interaction for establishing norms of worker gestures. Conversely, it can also use the same power meter via an energy desegregation technique in identifying the power levels and states of machine individual components as causes to observe effects of worker responses via video cameras. This study serves as the first step towards the causality-inspired contextual WMI recognition system. This paper presents a case study of semiconductor fabrication processes to demonstrate the capability to capture the sequence of contextual machine events with WMI contexts. In addition to the use of FSM modeling for the timing and causal behaviors of workers and machines, a novel energy disaggregation technique by exploring the logic states of machine components and their corresponding working principles is researched for analyzing power signals with fast-varying pulses caused by bang-bang control at a low sampling frequency, resulting in identification of power signature of individual components at various state. Finally, the contextual awareness of anomaly detection of workers and machines is illustrated.

2. Related Work

2.1. Context-aware Manufacturing Systems and CPS

Context-aware manufacturing systems have become a vibrant research area recently. Several studies focus on system-level designs by using IoT-based multi-sensor fusion and ML to achieve context-awareness [10, 11, 12, 13]. For example, Alexopoulos et al. utilizing massive sensor data designed a context-aware information distribution system that has visibility of shop floor processes and provides relevant recommendation information to relevant people [14]. In addition, the existing knowledge from humans can be provided to assist the design of a context-aware system. Horváth conceptualized a context-driven and knowledgedriven CPS modeling and system design methodology [15]. Emmanouilidis et al. proposed a conceptual context-based framework for maintenance management that integrates expert knowledge to a classification model where humans can identify unknown data or conditions and subsequently include the unseen information into a knowledge pool for future uses [16]. Wang et al. leveraged the known contextual information about a CNC machine to classify the collected data from CNC and mounted sensors into different machine states [17]. Inspired by these previous research work, this paper further leverages the documented knowledge from interaction-based SOP and the instrumentation working principles of machines in the software design phase to expedite the contextual system development in CPS.

2.2. Machines and Their Components Monitoring

Technologies for monitoring multiple machines status have been reported using RFID [25, 26], Wireless Sensor Networks [27, 28], or interfacing with PLC [29]. On the other hand, the component characteristics of an individual machine in real time is information of interest for gaining its operation visibility, since in general a manufacturing machine has multiple components (e.g., pump, heater, spindle). Drake et al. proposed a framework to characterize the energy consumption of machines and their components in real time by utilizing one power meter to monitor the total power of an individual machine and by analyzing its components' power based on the prior dataset collected from operating the components in a sequential order [30]. Panten et al. correlated the machine condition data from PLC with aggregated power data to identify the energy consumption of machine components in an online manner [21]. Tan et al. correlated the production data with power consumption to monitor machine status in real time [31]. Cheng proposed an alternative by monitoring machine operation states through current analysis eliminating a need to interface with PLC [22]. Han et al. discussed using non-intrusive high-frequency audio and vibration signals to classify faults of a cutting machine [32]. In this paper, a knowledge transfer CPS is proposed to address both machine and components monitoring. The hardware uses a combined camera and power meter for the real time visual and energy information respectively. The software facilitates

Table 1A comparison with some previous work

Ref.	Year	Monitoring	PLC/Intrusive	Submetering	Technology Description	Context-aware
[18]	2020	Yes	Yes	N/A	MTConnect+Petri Net	No
[19]	2020	Yes	Yes	N/A	Combined with Digital Twin	No
[20]	2020	Yes	No	N/A	Computer vision based panel recognition	No
[21]	2016	Yes	Yes	No	Energy disaggregation with PLC control variables	No
[22]	2018	Yes	No	No	Frequency spectrum signal analysis	No
[23]	2019	Yes	No	No	Kalman Filter	No
[24]	2020	Yes	No	Yes	Supervised machine learning	No
Ours	-	Yes	No	No	Knowledge enhanced unsupervised way	Yes

the correlation between the finite states defined by interaction-based SOP and the real time visual and energy information. As listed in table 1 comparison with several previous studies of using PLC or energy states [18, 19, 20, 21, 22, 23, 24], this novel approach can be easily implemented without requiring interfacing with customized PLC, massive sensors, and laborintensive dataset collections for model training. Furthermore, with the correlated SOP model and visual information from cameras, WMI contexts can be extracted effortlessly.

2.3. Energy Disaggregation In Machines and Their Components

With a great number of non-intrusive load monitoring (NILM) solutions for energy disaggregation being developed and evaluated on residential applications in recent years [33], researchers have begun to explore its potential in industrial sectors [34, 35]. There are typically three types of loads: single state (on/off), multi-state, and continuously varying [36]. Energy event detectors serve as major modules for the first two types to extract steady-state features, and the third type demands high sampling rates at kHz for capturing transient and high-order harmonics features [37, 38]. Several window-based event detectors are proposed by studying statistical features, e.g. Chi-squared test [39], generalized likelihood ratio detector [40], Teager–Kaiser energy operator [41], variance and absolute deviation[42]. Many of the existing energy event detectors are evaluated on kHz signals or less oscillating signals for residential appliances, whereas in this study we develop a detector on low sampling rate signals superposed with fast-varying pulses for manufacturing equipment. Furthermore, we explore the use of human knowledge in instrumentation designs for machine component control such as temperature, spinning, heating, flow, etc., and their corresponding electrical signatures for energy disaggregation. This is done by correlating a main power reading from FSM-based SOP with electrical signatures of components to identify the power consumption of individual components. It is of interest to note that the main power reading is a result of context awareness of repetitive measured signals from a main power meter. While beyond the current scope of this paper, it is worth mentioning that the same methodology can be easily extended towards energy disaggregation of multiple machines for an entire manufacturing floor with a single power meter.

2.4. Operator **4.0**

In the context of Industry 4.0, several frameworks of operator 4.0 have been proposed to empower workers' capability, monitor workers' behaviors, and identify operators' new roles. For example, Segura et al. introduced visual computing technologies to assist worker operations [43]. Zolotova et al. discussed how operators and cyber-physical production systems interact with new trending technologies [44]. In addition, Kaasinen et al. analyzed user expectations and worker concerns regarding the adoption of operator 4.0 technologies [45]. Cimini et al. conceptualized a human-inthe-loop framework to discuss humans' critical roles in interactions and enhanced decision making with manufacturing systems as a socio-technical system [46]. In this work, the contextual sensor system will enable the real time training of machine operation for workers, the operational fault detection, and the prevention of occupation injuries, since the WMI are constantly under surveillance in a non-intrusive manner.

3. Contextual Sensor System Design

As depicted in figure 1, the proposed contextual sensor system is based on an FSM model built from the SOP including workers and machines, which are correlated through state transition functions. The system hardware consists of a visual camera and a power meter to collect real-time data, and a contextual software to process the sensed contents to generate contextual information. The system implementation incorporates a knowledge transfer framework that leverages human knowledge and documented knowledge to initialize the contextual software design with these two simple sensors. A case study of a semiconductor fabrication machine is successfully demonstrated using the proposed contextual sensor system hardware and software architecture.

3.1. A Context-Centric SOP Model and Knowledge Transfer Framework

For a single manufacturing machine or workstation, the standard operation procedures (SOP) provided by equipment vendors define a sequence of operations a worker needs to accomplish, which can be modeled as a sequence of interactive events $\{e_0, e_1, ..., e_n\}$. The interactive events define the actions or information a worker needs to take and the expected result a machine will provide, which forms cause-effect pairs. The contextual information underneath an event

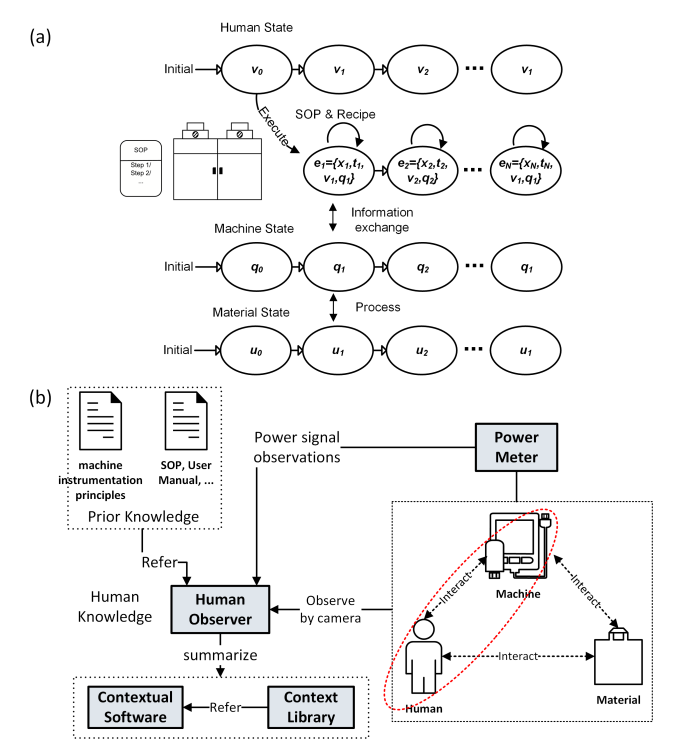


Figure 1: (a) An example of the FSM-based SOP model abstraction. The SOP defines an event-based operation sequence with worker state and machine state. Material state is changed by machine processing via a recipe developed by human. In (b), the proposed knowledge transfer framework in CPS. Note that this paper focuses on the worker machine interaction only.

can be modeled as $e = \{x, t, P\}$, where x is the location, t is the timestamp, and P represents the event properties including both sides (workers and machines). The worker and machine status can be modeled as a Finite State Machine (FSM) respectively to represent the consistent state transition. The SOP provides such state transition information as shown in figure 1(a). The machine (or its component) states qcan be the operation states such as off, standby, on, and material loaded etc., and the worker states v can be operating actions. It is worthwhile mentioning that the operation states of a machine include multiple functional instrumentation modules, i.e., heating, pumping, spinning, etc., which are independently processed by various machine components and can operate in sequence or simultaneously. The machine states and worker states are correlated through the transition function δ defined by SOP as

$$q_{i+1} = \delta(v_i, q_i), q \in Q, v \in V \tag{1}$$

where Q and V are the predefined machine state space and worker state space from SOP respectively. The SOP event context becomes $e = \{x, t, v, q\}$, in which the machine state change is a result of different worker states. For example, a manually controlled machine is turned on because a worker presses the switch a few moments ago. By using this correlated SOP model as the basis, machine events and worker events can be detected independently and correlated

uniformly to uncover the WMI contexts. In this study, we focus on the machine energy state determination.

In addition to the related worker and machine state transitions, materials can also transit their states *u* after a worker controls a machine to process. The material state transitions can be additive or subtractive to a part (e.g., wafer) to show shape changes, phase changes (e.g., metal refining from solid to liquid), or chemical reactions with byproducts. The material state transition can also provide the contextual information similar to the WMI but is beyond the scope of this study.

The correlated SOP model serves as the basis of the knowledge transfer framework and the contextual sensor system. The correlated SOP model defines two entities to be measured, worker states and machine states. In order to capture signals from both sides, a visual camera (can be a security camera) and a power meter are selected as the hardware sensors for the contextual sensor systems. Visual Cameras are readily available sensors and contain meaningful contexts of workers and surroundings, which are selected to determine worker states and side channel information from the surrounding environments and machines. On the other side, the machine or component energy state change can be directly reflected on the energy consumption, which is measured by a main power meter in real time.

Based on the SOP model, a knowledge transfer framework is built to define a workflow to transfer the implicit engineering knowledge from workers and documented prior knowledge to the system design loop as illustrated in figure 1(b). Basically, a shop floor includes three major elements: people, machines, and materials, among which direct or indirect interactions occur to proceed the manufacturing processes in a way of state transitions. For example, machines interact with materials to process a recipe (e.g., deposition, etching) for changing product states [47]. A Worker interacts with a machine through an interface to control process parameters, start running processes, and change the machine state. A human observer is introduced in this framework to serve as a knowledge accumulator by watching the always-happening interactions through cameras in accordance with the SOP, instrumentation principles, and the sensed power signals. In fact, the human observer can be senior process engineers and does not need to in-person watch the process since the engineer has already established their knowledge database during the long-term career. Initially, with prior knowledge, the human observer is to acknowledge the variation of power signals by analyzing the recent observable interaction sequence with corresponding power outputs to confirm the relevance and consistency among SOP, power signals, and realistic human-machine interactions. The observer can follow the SOP to recognize the worker state (from WMI) and thus understand the corresponding machine state and power signals. The corresponding segment of power signals can be attributed to a certain component or a group of them with respect to the SOP. Finally, the obtained and summarized knowledge from this observation can be leveraged and transferred to boost and append the context extraction

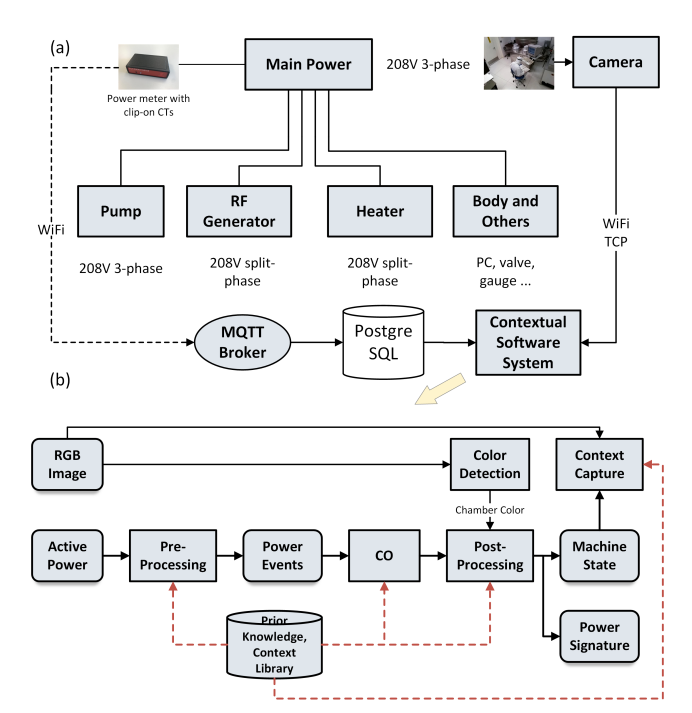


Figure 2: The hardware and software structure of the implemented contextual sensor system. (a) shows a semiconductor processing machine, the PlasmaTherm with 4 instrumentation modules (see the text) with their corresponding components connections with various power supplies. A visual camera is mounted from a near ceiling view to monitor the entire machine. (b) outlines the data processing pipe.

capability to the software design process. After few iterations, a contextual sensor software can be developed to act as an artificial human observer to recognize component state transitions from aggregated power signals. Moreover, the knowledge of human observer can be abstracted and encoded into a context library where several known consequences of the interaction processes and events are stored, and which can be used as a look-up database to search for possible reasons when some typical sequences of events are detected. The proposed knowledge transfer framework based on the correlated SOP avoids the submetering data collection to identify component power signals. It is also noted that the deviation of typical sequences of events could be used to identify anomalies of machine operation, which might be attributed to gradual performance degradation of functioning components or undetected intrusions in cyber-attacks.

In addition, with many component state transitions being detected, the WMI videos can be annotated in a label-free manner according to the FSM-defined state transition correlation to train a ML model to recognize the interactions, which will be addressed by another publication from the authors.

3.2. Contextual Sensor System Architecture

We applied the proposed knowledge transfer framework to develop and implement a contextual sensor system on a typical semiconductor fabrication equipment, PlasmaTherm,

Table 2A generalized SOP of PlasmaTherm with dual functions

Step	Process		PECVD		RIE			
Step	1 Tocess	Pump	RF	Heater	Pump	RF	Heater	
1	Set temp.	on	STBY	on	-	-	-	
2	Vent	on	STBY	on	on	STBY	off	
3	Load	on	STBY	on	on	STBY	off	
4	Pump down	low vac	STBY	on	low-vac	STBY	off	
5	Run Process	on	on	on	on	on	off	
6	Purge & Vent	on	STBY	on	on	STBY	off	
7	Unload	on	STBY	on	on	STBY	off	
8	Reset temp.	on	STBY	off	-	-		
9	Pump down	low vac	STBY	off	low vac	STBY	off	

located in a cleanroom facility. PlasmaTherm is a PLCcontrolled machine with dual chambers and functionalities: PECVD (plasma enhanced chemical vapor deposition) and RIE (reactive ion etching), by using the generated gas plasma. Several gases can be used to generate plasma for different purposes. The machine is equipped with multiple instrumentation functions: the creation of desired vacuum conditions for semiconductor processing, the generation of plasma from gases and RF sources, the control of semiconductor substrate temperature, the electronics for PLC and user interfaces. These instrumentation functions have corresponding components: mechanical vacuum pump (roughing pump), RF generator, heater with controller, and main body with PLC and PC etc., respectively. These components can be in various states at each process step for different functions. The two processing chambers are driven by the same set of components. RIE side does not require an elevated temperature setting, while PECVD requires a constant elevated temperature during deposition. The simplified and generalized SOP for the two functions is illustrated in Table 2 (STBY stands for standby states, and low-vac represents the chamber lowvacuum states). A worker is required to execute the SOP through the machine interface (a monitor with keyboard). For example, at step 5 a worker operates the keyboard to choose a product recipe and hits "RUN" button to start the process, which results in the RF state changed from standby to on when the inflow and removal rate of gases (by vacuum pump) reach a steady state.

Figure 2(a) depicts the hardware and data acquisition and transmission settings. A visual camera is mounted to capture the real-time image stream through WiFi connection and TCP protocol. The image size is set to be 640×480 with the frame rate of 10 fps. A clip-on power meter with current transformers (CTs) are installed on the circuit breaker to monitor the main power feed for the entire machine. The meter we used is easily installed by clipping on the CTs to the power lines with voltage sensing wires connected to the power lines. The meter is reconfigurable to monitor threephase, split-phase, or single-phase load. Since other singlephase components, e.g., PC, PLC, and valves, consume less power and maintain insignificant power change compared with main parts, they are omitted in this study. The power meter samples the active power signal at 1 Hz frequency and transmits JSON-format data through MQTT, the data is stored in a local PostgreSQL database. The developed contextual

 Table 3

 PlasmaTherm power states and corresponding response time

Name	Attr.	States								
			off		on					
Body	Power (W)		0			900				
	T_{res} (s)		-			1				
			off							
Heater	Power		0		1300					
	T_{res}		-		30					
		off		(on	low vac				
Pump	Power	0	7		50	1100				
	Tres	-		-		2				
		STBY	30W	70W	125W	175W	300W			
	Power	50	300	400	500	600	850			
RF	$T_{res}(CF_4)$	-	90	90	90	90	90			
	$T_{res}(O_2)$	-	65	65	65	65	65			
	$T_{res}(SiH_4)$	-	215	215	215	215	215			

sensor software system queries the database every second to fetch the power data and accepts the real-time image stream to process.

The data processing pipeline is illustrated in figure 2(b). There are two streams for the image data and power data processing respectively. The power data processing stream analyzes the main power to extract different types of power events and disaggregate them to derive the individual component states with predicted individual signals. The details of this power signal processing will be addressed in section 4. Since the visible light emission depends on the type of gases in use for plasma, a color detection module based on the chamber window color intensity is developed to detect the plasma gas type. With the contents of power signatures and chamber color detected, a context capture module is developed to correlate the contents into contexts.

Since the SOP model defines the correlation between machine states and worker states as visible in WMI video snaps, one design aspect of the captured context is the response time T_{res} between WMI and machine state transitions. The response time is common for PLC-controlled manufacturing machines to conduct a self parameter inspection or adjustment before a process starts. Using PlasmaTherm as an example, when a user selects the processing recipe and hits the "RUN" button, the machine will first adjust the gas flow rate to reach steady states for a fixed period of time after which the RF is turned on and the manufacturing process begins. The corresponding response time is composed of a static segment and a transitional period depending on the gas flow. The response time for PlasmaTherm is listed in table 3, where T_{ros} is derived from its inactive state (heater: off, pump: on, RF: STBY) to operational (active) states. RF has three T_{res} distinctive on the gas type since the gas flow rate and the time to steady states are different. In reality, since the gas flow rate varies, T_{res} can be regarded as a normally distributed random variable depending on multiple factors (e.g., gas valve leakage, gas inventory, pressure). After several iterations in measurements, an averaged response time over measurements is selected as T_{res} . If the interaction starts at time 0, the machine state change will be recognized at time $T_I + T_{res}$, where T_I is the interaction duration. Therefore, the time period $(0, T_I)$ containing WMI contexts needs to be pinpointed.

The other design aspect of the captured contexts is to analyze the sequence of detected events with timestamps and compare them with the context library to determine possible consequences. For example, following the expert experience, a 30-min oxygen clean should be conducted to clean the inner chamber before any etching or deposition process begins. If a worker forgot to do it and failed to obtain the expected processed material, the contextual sensor system can provide a likely cause that the oxygen clean was not performed. Moreover, by comparing the duration or the magnitude of the low-vac state pump power signals, the system is able to estimate the efficiency of the pump or whether the pump or valves have unusual leakage. With the context library built upon expertise from humans and documented knowledge, the contextual information and actionable intelligence can be supported by the system. In this study, to illustrate the proposed framework, three predefined contexts are abstracted from facility staff's knowledge and SOP with reference to the event sequence: 1) A regular operation should follow a sequence of RF on (optional O2 clean), pump low-vac, RF on (can be multiple times), pump low-vac, and RF on (optional O2 clean), where over 60-minute continuous RF running is prohibited; 2) While it is rare that two consecutive pump low-vac states are detected, this sequence may indicate a pump malfunction during first low-vac state; 3) a small bump of the pump power signal during inactive pump on states can indicate an unusual gas leakage from the enclosed chamber, valves, or pipes.

4. Software Defined Sensor for Power Event Detection and Classification

In this section, the prior knowledge from SOP and the working principles of instrumentation engineering designs for functional modules are utilized to design the software defined sensor system, which is capable of detecting power events and reporting the individual components' energy consumption. As illustrated in the power signal processing in figure 2(b), it includes preprocessing, Combinatorial Optimization (CO), and post-processing. It is worthwhile mentioning that the knowledge of instrumentation principles and their corresponding components can highlight the anticipated power waveform during normal operation.

4.1. Working Principles of Functioning Instrumentation Modules and Their Components

4.1.1. Design of a Vacuum System

The rotary-vane vacuum pump, a type of mechanical pump, is typically used in semiconductor fabrication equipment as the roughing pump for creation of low vacuum. The pump is driven by a three-phase motor and its power consumption is related to the amount of gas in the enclosed chamber according to the working principle. When the machine chamber pressure is always low at idle states, e.g.,

10 mTorr, the power consumption of the motor is relatively constant and low. When the chamber is vented to atmosphere for sample loading and needs to be vacuumed again, the motor load increases abruptly, which will cause a power surge of the motor. With more gas being pumped out and lower chamber pressure, the motor load will gradually decrease, which reduces the power consumption to the constant level. From the prior knowledge about the working principle, we can derive an educated guess of the pump power signature during operation.

4.1.2. Design of RF Plasma Generator

RF plasma generators are pervasively applied in semiconductor fabrication to generate reactive gas plasma for dry etch, PECVD, and inert gas for sputtering etc. In general, a RF plasma generator includes a RF power supply, a RF matching network and a reactor (torch) [48]. The generation of gas plasma depends on the gas type, gas flow, pressure, temperature, humidity, and RF power [49]. One of the key processing requirements of the generated plasma is to maintain a constant plasma power and density to stabilize the etching or deposition process. Therefore, the power supply of the plasma generator is designed to provide a stable power during the process and can be tuned to control the generated plasma property. PlasmTherm has a PLC to control the process with stable RF power using predetermined process recipes, allowing a user to select a recipe with specific plasma power and duration.

4.1.3. Constant Elevated Temperature Controller

In many industrial applications, a stable temperature control is important for product yield and thus tools are equipped with self-regulating heaters. With thermocouples to sense temperature for a feedback control, a heater is designed to be turned on and off when the temperature is low or high respectively for stabilizing a preset temperature. At the beginning of ramping up the temperature from 25 °C to a user selected temperature, such as 250 °C, the heater operates at a constant power mode until the temperature gets close to the set value. During elevated temperature stabilization, a feedback control mode kicks in to turn the heater on and off frequently. Compared with other instrumentation functions, the pulse-like waveform is unique for the heater and the harmonic features can be extracted to detect such a pulse signal with higher-order frequency components.

The knowledge from these three instrumentation function modules will be explored in the design of data processing in software defined sensors for identification of three machine components, i.e., pump, RF generator, and heater.

4.2. Two-stage Data Preprocessing

In order to deal with the 3 components with similar or different power events, a hybrid two-stage algorithm is designed to pre-process the aggregated raw power signal and detect the power events of different types in real time. There are basically two types of power events, one for the pump, RF generator, and constant power heater with steady state features, the other for the heater in the pulsing mode.

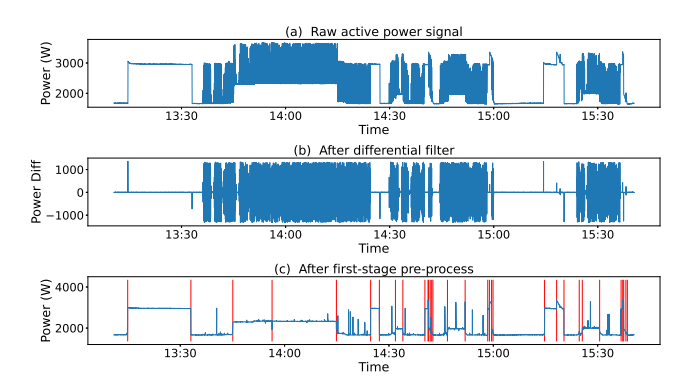


Figure 3: An example with the measured raw signal going through the first-stage preprocessing algorithm (based on the instrumentation functions) to show the performance. (a) an active power signal captured from the main power meter with heater, RF and pump at different states. (b) the signal after differential filter with signal variation being amplified. (c) the derived signal after first-stage pre-process to remove the pulses. The red lines in (c) indicates the detected power event from second-stage pre-process.

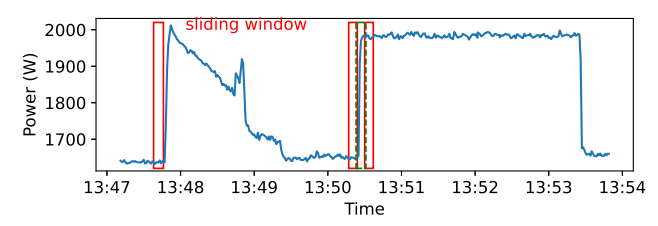


Figure 4: An illustration of a power signal with the SW-based second-stage preprocessing techniques to detect power events. In the middle, the two red boxes represent two windows right before and after the power ramp with the small variance, whereas the green dashed box represent the window capturing the edge with large signal variance. The two red windows also capture the steady state powers and the random noise or spikes can be avoided through comparison with steady power values.

Figure 3(a) shows a raw power signal captured from the main power meter during PECVD operation and consists of different combinations of the pump, RF, constant power heater, and pulsing heater at different states. There is a rather challenging case where the pump is in low-vac state and the heater turns on to the constant power mode and then transits to the pulsing mode or vice versa, increasing the difficulty to detect all types of power events. To overcome this challenging task, we segregate the detection of the two event types: pulsing states based on raw signals, and steady states based on filtered (removing the pulses) signals.

To detect the pulsing state from a raw signal, the raw signal is first partitioned into sliding windows (SW) with a width of 20 and a stride of 1. A differential filter is applied on the windowed signal to calculate the signal difference between adjacent timestamps, which can be represented as $P_d = P_{t+1} - P_t$. The frequency domain feature is calculated within the windowed P_d by Fast Fourier Transform (FFT). The 2nd and 4th order frequency components are extracted

and a threshold (th_{fft}) is applied to determine whether the signal includes fast-varying pulses.

With the capability of detecting the pulsing mode, one can remove the pulsing component and extract the remaining waveform for the steady state power event analysis. The complete two-stage preprocessing method is illustrated in Algorithm 1. When no pulses are detected by FFT, the raw signal value is kept in the filtered signal. When there is a pulse, a threshold (bound derived from the heater on-off power value in table 3) is applied on P_d to filter the fast-varying data points. The remaining signal is compared with the maximum possible value (th_{max} derived from table 3) at non-pulse states to determine whether to keep the raw value or subtract the heater on-state power from the raw value. Then the filtered signal P_f is derived. Note that the P_f is also experienced re-sampling as the fast-varying pulses are removed instead of filtered. Figure 3(b) and (c) show an example of signals after the first-stage preprocessing. We can observe in figure 3(c) most of pulses are removed and the steady-state waveform including RF, pump, and constant power heater is preserved. There are still a few non-filtered spikes in P_f , which can be eliminated in the second stage signal processing with a noise-tolerant feature.

The second stage of the preprocessing method is designed to detect the edges and steady state values from P_f . We apply a sliding window with a width of 5 and a stride of 1 on P_f as illustrated in figure 4. The signal variance of each window is calculated and a variance threshold (th_{var}) is applied to filter event windows and non-event windows. This is based on an assumption that in industrial environment power events do not happen more frequently than the window width. Therefore, two non-event windows with steady-state power values should be right before and after a series of continuous event windows. When the difference between these two steady state values is greater than a threshold (th_{ch}) that can be derived from the minimum power difference during any possible state changes in table 3, a power event can be determined, resulting in automatically eliminating the nonfiltered spikes (noise) to enhance the robustness. In addition, a complementary checking is included to always verify the current steady-state values during non-event windows to avoid any missing events.

4.3. Energy Disaggregation

The basic idea of energy disaggregation is to solve an optimization problem by using the power signatures of each device as

$$P_{agg}(t) = \sum_{m=0}^{M} P_m(t) + e(t)$$
 (2)

where $P_{agg}(t)$ represents the aggregated power signal, $P_m(t)$ is the individual component power signature, and e(t) represents the realistic power deviation from the power signature. In this study, the components (main body, pump, RF generator and heater) of PlasmaTherm are regarded as the individual device for disaggregation. The main body is always on and consumes 900W power. The other component states are

Algorithm 1: A Hybrid Two-stage Preprocessing and Event Detection Method

```
Input: P_{raw}, and predefined thresholds
Output: event type, time, steady state power, P_f
P_d = (P_{raw}[1:] - P_{raw}[:-1]);
freq_{mag} = FFT(P_d);
if freq_{mag} > th_{fft} then
    Output pulsing heater event;
    if abs(P_d[-1]) < bound then
         if P_{raw}[-1] < th_{max} then
             P_f.append(P_{raw}[-1]);
         else
             P_f.append(P_{raw}[-1] - HeaterOnPower);
else
    P_f.append(P_{raw}[-1]);
# Second Stage:
Calculate signal Variance var on P_f;
if var > th_{var} then
    eventFlag = 1;
else
    if eventFlag == 1 then
         s = mean(P_f[0:2]);
         if abs(s - s_{last} > th_{cb} then

Output event type, time, steady state
              power:
    else
         s = mean(P_f);
         if abs(s - s_{last}) > th_{cb} then
Output event type, time, steady state
              power;
    eventFlag = 0;
```

illustrated in Table 3. As process recipes set different RF power and processing time, the distinguishable power states include different RF power levels.

CO is a simple and generic technique for solving such a combination problem in the energy disaggregation field [50]. The basic idea of CO is to combine the possible power signatures to find the closest combined signal compared with the real aggregated signal. One drawback of the CO is that it only considers the steady state power values rather than a sequence of power signatures, which can cause misclassification when the power fluctuates beyond the allowable range or several combinations of the steady-state values are similar or even identical. In Plasmatherm example, the lowvac pump state has the same steady-state power as the 70W RF state, which cannot be resolved by CO. To distinguish this case, we leverage the prior knowledge about working principle differences. The power of pump low-vac state shows a time-varying decrease while the power of RF states is stabilized. We leverage this feature in the post-processing module to distinguish the low-vac state and the 70W RF

state and to disaggregate the pump signal with this specific ramp-down waveform. Furthermore, the deviation e(t) is distributed to individual components by considering the instrumentation working principles and operation sequence. The SOP provides the sequence of components being turned active and the prohibited combinations of active components. For example, active pump and active RF are not allowed to occur simultaneously, which is used to distribute e(t) when a component is active. By doing so, the individual component power signal is recovered.

5. Experiment Results and Discussions

The proposed contextual sensor system is evaluated by using PlasmaTherm and demonstrates its capability of the power signal pre-process and machine event classification with the WMI context extraction. In addition, we tested the disaggregation method on another machine (E-Beam) to further validate its performance.

5.1. Machine Event Detection and Disaggregation.

We tested the proposed method on three different cases: PlasmaTherm for PECVD, PlasmaTherm for RIE, and Electron Beam Evaporation (E-Beam) tool, to show the effectiveness of the machine event detection and disaggregation.

5.1.1. PlasmaTherm for PECVD

We deployed the contextual sensor system on PlasmaTherm to extract events without human interventions. It is noted that the extracted events of PlasmaTherm represent the power events of steady state transitions, including pump, RF, and constant power heater. The pulsing mode power events will be pointed out separately since the pulsing events do not involve WMI but are attributed to the automatic temperature control. Figure 3(c) plots the filtered signal during a PECVD process with SiH₄ gas and several O₂ clean involved. There are 28 power events during this process and the software defined sensor algorithm detects 34 power events including all the 28 ground truth power events with additional 6 events. The extra detected events do not affect the disaggregation result as they are not classified as machine state transitions in disaggregation.

To evaluate the energy disaggregation performance, we collect the actual individual power signals for each component as the ground truth data. Figure 5 depicts a typical segment of the machine event detection and component energy disaggregation results in PECVD case. The specific waveform of the pump is successfully disaggregated. For the RF signals, there are relatively small deviations between the ground truth and disaggregated data since in practice the RF generator needs to adjust its power slightly depending on operational conditions to maintain the generated plasma power constant. Figure 5(e) displays the disaggregated signal for the heater observing that the constant power heater signals are recovered. For the pulsing mode heater, the proposed approach can identify the start and end of the pulses with the capability of roughly extracting the pulsing heater signal.

5.1.2. PlasmaTherm for RIE

Figure 6 illustrates an example of a RIE process performed in PlasmaTherm, where RIE does not require elevated temperature setting but in fact heater is active for a few seconds. The reason is that during non-PECVD processes including RIE and machine standby, the heater temperature is set to be 23 °C close to the cleanroom temperature. When the thermocouple detects temperature deviations (below 23 °C), it will trigger the heater to be on, resulting in several spikes in the heater power and main power. Other spikes belong to noise from the CTs. Without the pulsing heater involved, power events in RIE are easier to recognize than those in PECVD. Figure 6(b) and (c) show the successful disaggregation of power signals for the pump and RF during RIE respectively.

From Feb. 19, 2021 to Mar. 24, 2021, there are 17-time PlasmaTherm usages with 15 for RIE and 2 for PECVD. In total 103688 data points (around 29 hours) of raw signals during active machine usages are collected from a power meter. Table 4 lists the usage information during this period with time, process, the number of events (in the column, the values stand for pump, RF, and constant power heater in order), the number of detected events, and the number of data in active modes for each component. To provide a quantitative evaluation, the mean absolute error (MAE), root mean square error (RMSE), and mean percentage error (MPE) are calculated for comparing predicted signals and ground truth signals. Table 4 also shows the MAE (Watt), RMSE (Watt), and MPE (%) of each usage with the average values of all the data points. Since the heater signals have 0 values which cannot be used to calculate MPE, MPE is omitted for the heater. In total there are 47 pump events, 67 RF events, and 11 constant power heater events, and they are all successfully detected and classified by the proposed method with related event contexts being extracted. During each usage, the active RF states account for most of the usage time and power consumption as workers prefer running long-time oxygen clean before and after the process. For the PECVD processes, even though there are in total 11 constant power heater events, in practice a user only sets the temperature once at the beginning and the rest of the constant power heater events are due to the temperature change when a user opens chamber to load and unload a semiconductor wafer and thus decreasing chamber temperature sharply.

An interesting observation can be derived from table 4. An average time for pumping down during RIE can be derived which is 66.6 second. However, the mean pumping down time of usage ID 11 is 90 second, which is significantly longer, indicating a possibility of lower efficiency in the pump or a virtual leak in the machine. It is noted that the time information extracted from power events with our proposed contextual sensor system, e.g., time for pumping down, can be used as a reference for the system to identify unusual pump behaviors, which is of great context value in operation.

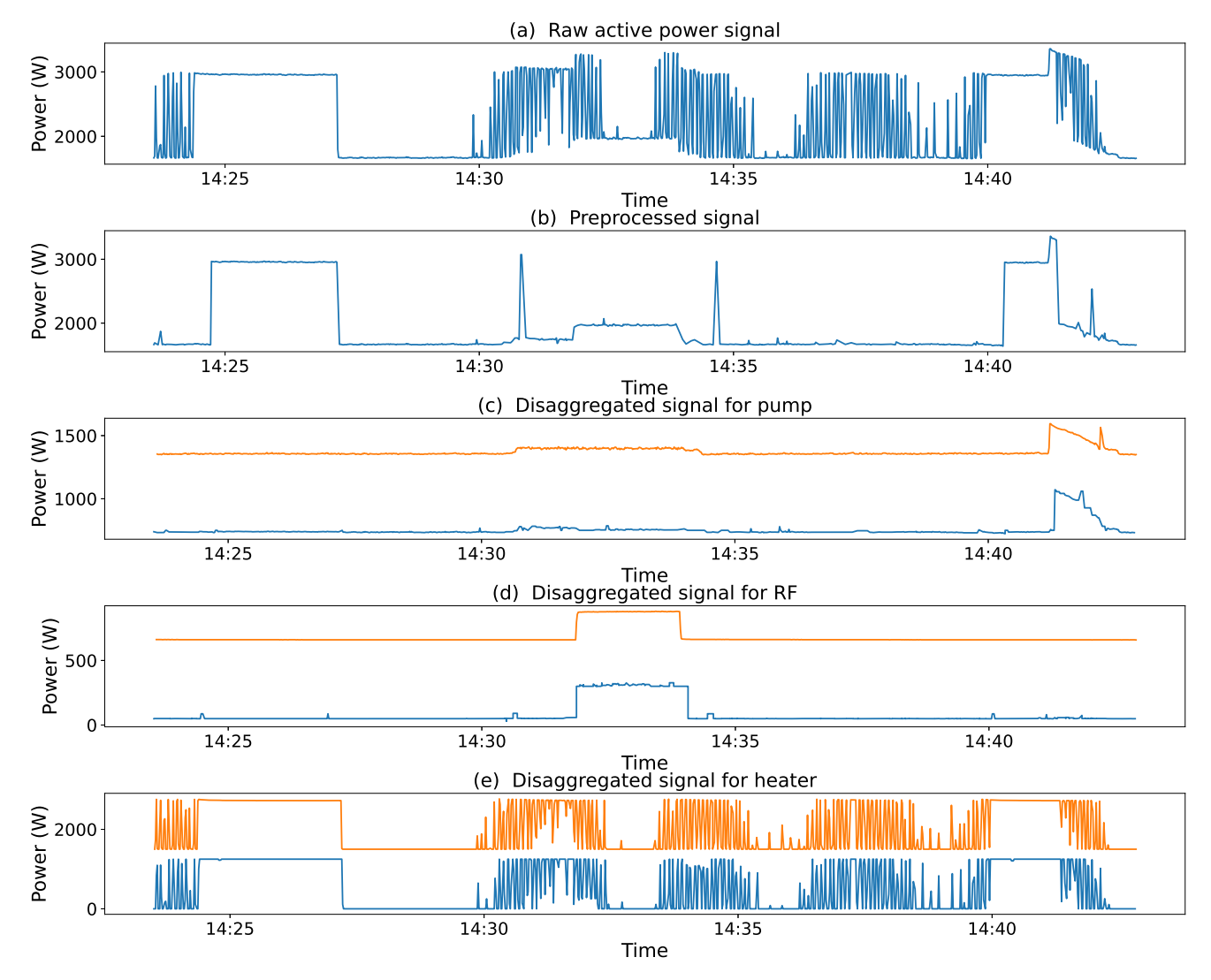


Figure 5: An example of the measured raw power signal during a PECVD process and its disaggregated component signals. (a) the captured raw signal with pump, RF and heater being active. (b) the signal after removing pulses by the first stage of preprocessing. In (c), (d), and (e), the disaggregated component signal (in blue) and the ground truth signal (in orange) are plotted for pump, RF, and heater respectively. Orange lines are lifted for better views.

Table 4
Usage information of PlasmaTherm with detected component events results

ID	Time	Process	#data	#evt	#det. evt		Pu	mp			F	RF			Heater	
10	Time	1 100033	#-uata	#-EVI	#uet. evt	#act.	MAE	RMSE	MPE	#act.	MAE	RMSE	MPE	#act.	MAE	RMSE
1	02/19 10:12-11:53	RIE	5478	2, 5, 0	2, 5, 0	118	28.6	31.7	3.6	1809	11.7	40.9	13.2	41	4.5	50.3
2	02/23 13:40-16:05	RIE	7448	0, 8, 0	0, 8, 0	0	24.5	25.4	3.1	3787	16.3	40.0	13.6	51	5.9	52.5
3	02/24 11:35-12:25	RIE	2441	2, 2, 0	2, 2, 0	117	32.3	35.8	4.0	1694	10.6	34.3	7.6	14	6.9	52.4
4	02/25 09:17-10:00	RIE	2318	2, 2, 0	2, 2, 0	110	34.3	38.1	4.3	1358	15.5	35.2	10.0	18	6.8	54.4
5	03/01 10:00-14:00	PECVD	12010	6, 5, 5	6, 5, 5	542	33.5	40.6	4.2	5520	37.1	58.1	18.9	5895	367.4	596.4
6	03/10 14:14-16:14	RIE	6384	4, 4, 0	4, 4, 0	227	21.9	27.1	2.8	2411	21.2	45.1	14.9	25	4.8	47.1
7	03/11 11:18-14:15	RIE	9197	4, 5, 0	4, 5, 0	222	23.5	27.4	3.0	3758	16.2	32.7	13.2	82	2.5	31.3
8	03/11 15:06-15:21	RIE	818	2, 1, 0	2, 1, 0	115	30.3	39.8	3.7	55	14.0	48.2	17.8	5	7.4	54.9
9	03/11 15:57-17:21	RIE	4620	2, 4, 0	2, 4, 0	118	22.0	25.3	2.8	1956	17.9	46.8	13.7	31	4.3	40.6
10	03/15 09:43-11:07	RIE	4504	3, 4, 0	3, 4, 0	191	23.8	28.4	3.0	1738	17.8	36.5	14.7	41	6.5	51.3
11	03/15 11:08-12:32	RIE	4618	2, 3, 0	2, 3, 0	180	21.6	25.7	2.8	3026	17.7	39.3	10.5	37	5.8	48.1
12	03/16 11:36-13:06	RIE	4616	2, 3, 0	2, 3, 0	131	22.3	25.8	2.9	3136	15.6	34.8	8.8	41	2.7	33.6
13	03/17 13:10-15:40	PECVD	8184	4, 4, 6	4, 4, 6	275	21.3	25.7	2.7	2321	24.9	50.1	18.7	3753	165.5	367.0
14	03/19 12:48-17:18	RIE	14439	3, 5, 0	3, 5, 0	257	23.7	27.3	3.1	5015	37.6	40.1	16.5	95	5.3	54.0
15	03/22 12:12-13:50	RIE	5454	3, 6, 0	3, 6, 0	232	24.4	30.0	3.1	3000	20.3	44.7	13.9	49	4.9	45.2
16	03/23 13:05-15:37	RIE	8259	4, 4, 0	4, 4, 0	307	22.1	26.4	2.8	3662	16.7	30.9	13.1	49	4.9	45.6
17	03/24 13:21-14:14	RIE	2897	2, 2, 0	2, 2, 0	140	24.6	29.3	3.1	1629	14.4	39.5	11.5	21	6.3	51.8
18	Mean	-	-	-	-	-	25.6	30.0	3.2	-	18.3	41.0	13.4	-	36.0	98.6

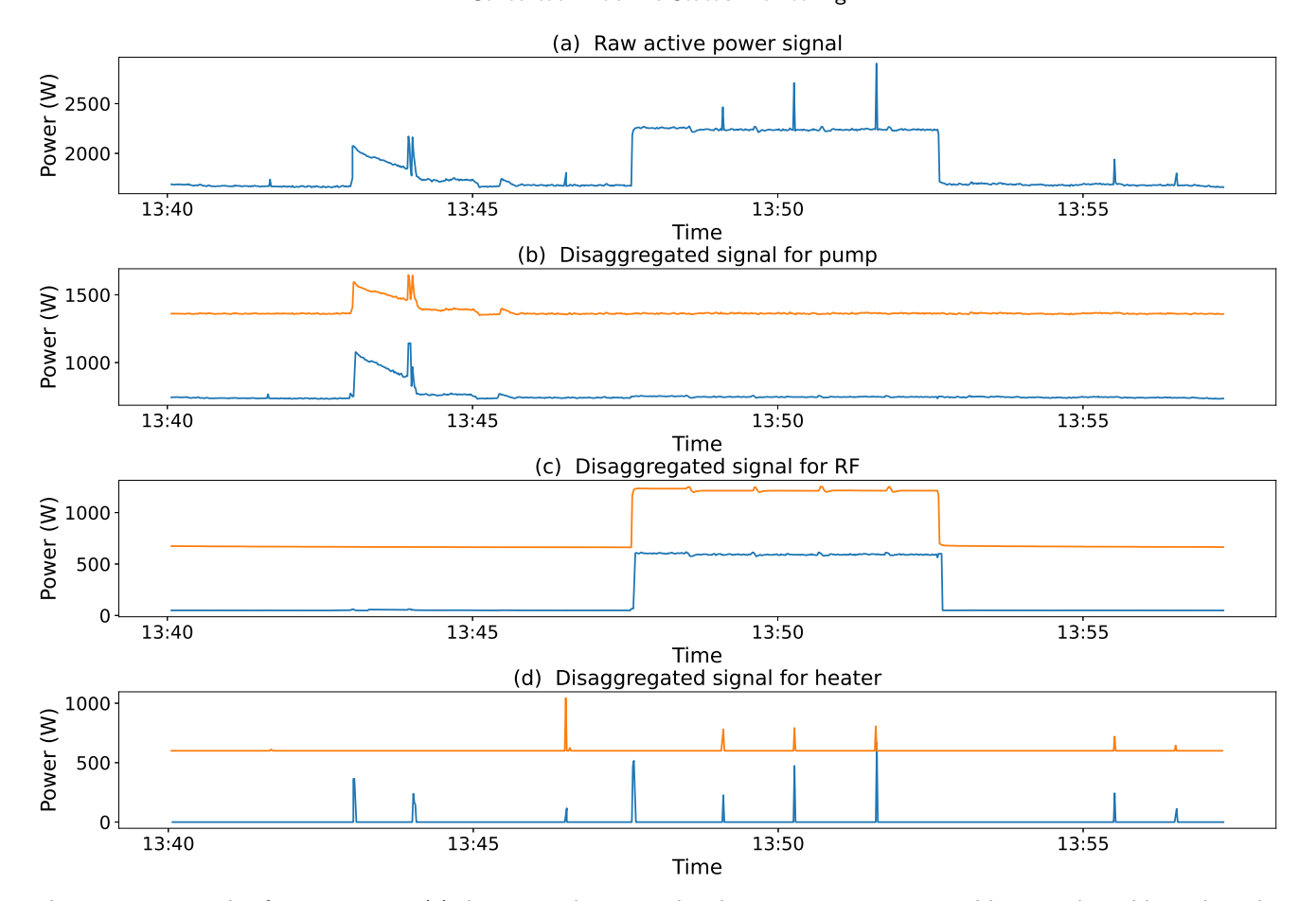


Figure 6: An example of a RIE process. (a) the captured raw signal with pump, RF generator, and heater. The red lines show the detected power events. In (b), (c) and (d), the disaggregated component signal (in blue) and the ground truth signal (in orange) are plotted for pump, RF and heater respectively. Orange lines are lifted for better views.

5.1.3. E-Beam

To evaluate the usability of the proposed machine event detection and disaggregation method, we further test the contextual sensor system on an E-beam deposition tool with Pump, Electron-gun (E-gun) and Controller as components for metal thin film deposition. This E-Beam is chosen not to be equipped with a PLC, i.e., manually controlled. The E-gun serves as the major processing component to provide high-voltage electron beams to melt metal and its current is adjusted manually by a worker using a built-in current meter. A simplified SOP of E-Beam is venting, hoist up, hoist down, pumping down, turning on controller, turning on E-gun, turning off E-gun and controller, venting, hoist up, hoist down, and pumping down again. The pump controls the vacuum steps, and the controller controls the hoists. Compared to PlasmaTherm with PLC, the processing time for E-Beam is manually controlled by a worker meaning that more WMIs are needed to turn off any active components as opposed to a PLC-controlled machine turning off active components automatically. Similarly, from the knowledge of human observer and SOP regarding the WMI sequence and measured power signals, the contextual sensor system is initialized on E-Beam. We used the same algorithm in Section 4 but adjusted the threshold parameters to better

accommodate individual components. To disaggregate E-gun power signals in the post-processing module, we applied the SOP knowledge that the E-gun will be turned on after controller is turned on. The disaggregated power signals from the measured raw signal are plotted in figure 7. In figure 7(d), the two spikes around 13:00 correspond to the hoist-up and hoist-down steps for loading and unloading wafers, which are successfully detected. This experiment further validates the effectiveness of the proposed method.

5.2. WMI Context Capture

Since PlasmaTherm is a PLC-controlled machine, the fabrication process can be turned off automatically depending on the process time set by users. Only the positive leading edges, which indicate a component transits from inactive to active modes, can trigger the WMI context capture. There is a distinctive worker gesture difference between changing pump state and RF state as illustrated in figure 8 that the worker tends to put their hand on the chamber handle to push down when performing the chamber pumping down. This is because the chamber cannot be completely sealed by its own gravity and hence requires extra force to push down. This distinctive WMI context is useful as well. For example, when a worker finishes the process and conducts the pumping down

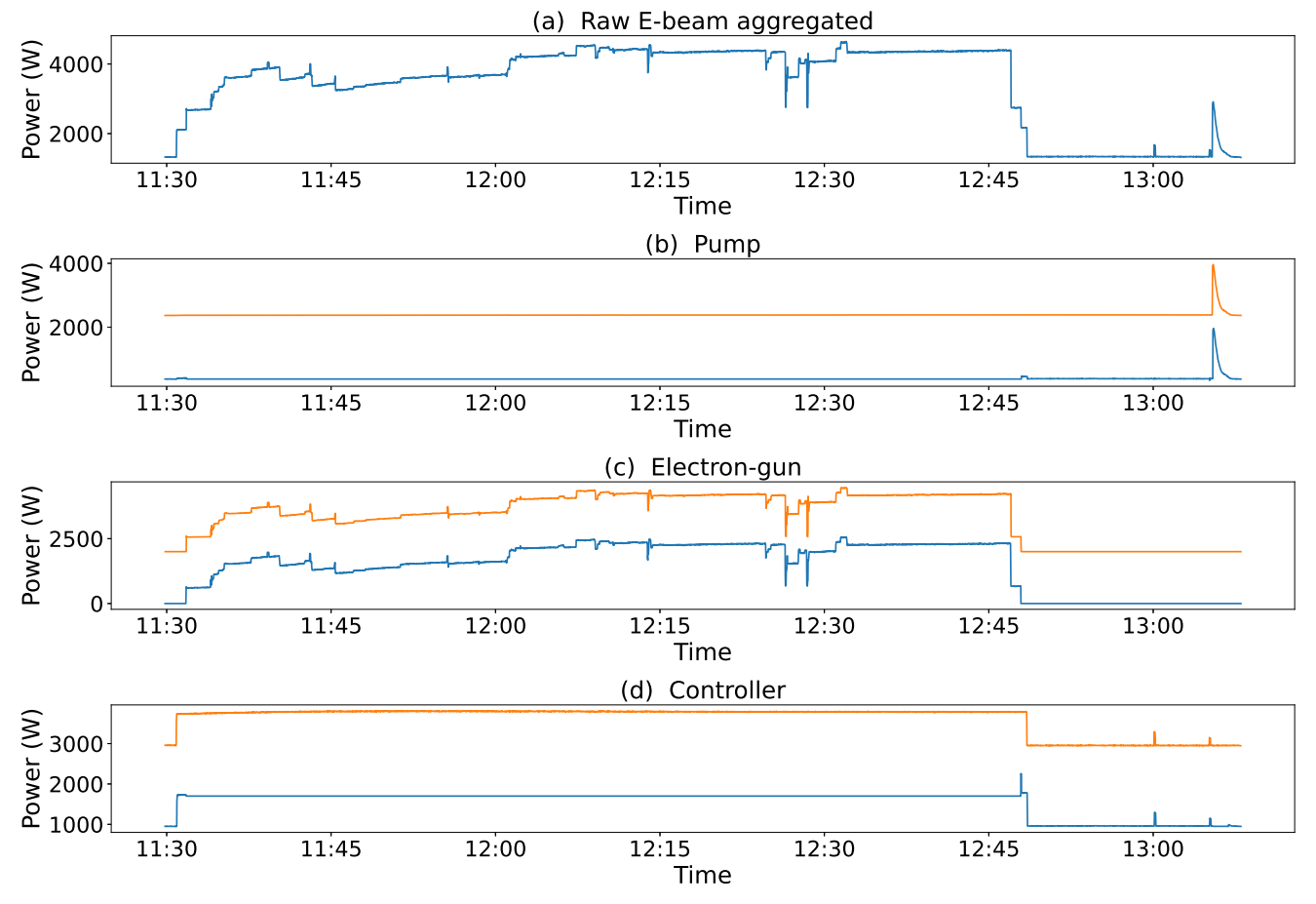


Figure 7: An example of a manually operated E-beam metal deposition tool is shown. (a) the measured raw E-beam signal. (b) to (d) the disaggregated (in blue) and ground truth (in orange) power signal for pump, E-gun, and controller respectively. The orange lines are intentionally lifted by 2000 W to keep the curves apart for easier views.

again to keep the chamber under vacuum for protecting its integrity but he/she forgets to push down the chamber handle to tighten the gap, the gas in the chamber cannot be vacuumed to the set pressure. With the WMI context being captured and recognized, this information can be provided to the user to check the machine chamber status and to avoid this incorrect operation.

5.3. Event Sequence Context Capture

Figure 9 illustrates an example of the first type context the system can capture, which is a typical machine usage following SOP. During this usage, a user first conducts a 30-min oxygen clean using 300W plasma power, then opens the chamber to load a wafer and conducts pumping down. A 70W oxygen photoresist ashing process is carried out for 1 minute in the RIE chamber, after which the user opens the chamber to take out the wafer and pumps down again. At last, another 30-min oxygen clean at 300W is applied to clean the chamber for the next user. During this operation, the component state with realistic power, the recipe information (including gas type, running time and plasma power), and the sequence of the operation are extracted and stored in a database. Accordingly, the WMI video clips during each interaction are captured and saved in the local file system

according to the response time of each component and gas type.

Figure 10 shows a captured example of a combination of the second and third type context related to pump issues. After a typical RF process, a user conducts pumping down as usual after which an irregular bump is detected by the contextual sensor system. Then, a second pumping down is conducted again by the user. The corresponding contexts during this period are captured. After the first pumping down, from the monitor the user noticed abnormal pressure value and informed the facility staff. From the disaggregated pump power signal, the bump corresponds to the abnormal pressure noticed by the user, which indicates that the gas inside the chamber is not vacuumed to the expected pressure and the air-tightness of the vacuum system is likely faulty. After a second-time pumping down, the pressure becomes normal. The extracted context is saved in the database and can be used as a reference when the same event sequence is met. One of the significances of this captured context is to be potentially used to conduct predictive maintenance and anomaly detection in the future.



Figure 8: Example images of interaction with PlasmaTherm by different users captured through WMI context capture process. The right column shows different interaction gestures to initiate pump or RF generator. Upright is referred as pump action and bottom right is RF action. The upleft indicates the locations of the smart meter installation and the chamber windows used for plasma color detection.

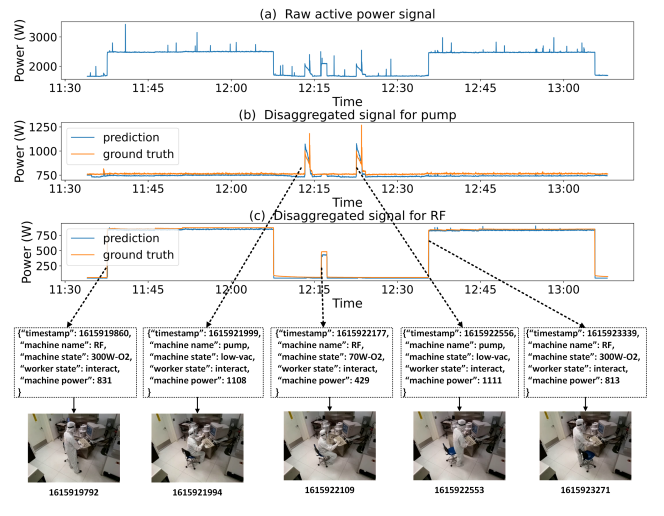


Figure 9: A first type of captured context during a RIE process is illustrated. The measured main power signal with disaggregated signals and ground truth signals are plotted. The heater signal is absent as RIE does not need heater. 5 positive edges correspond to 5 events with components from inactive mode to active modes. The extracted event contexts with UNIX timestamp, machine (component) name, state and actual power, and worker state are formulated in a JSON-format. The 5 corresponding WMI contexts are shown with the captured timestamp.

5.4. Comparison and Discussion

Comparison: To further validate the efficacy of the proposed machine event detection methods, we compared our method with some typical previous work with only the machine event detector replaced. We further tested on more data: 80 pump events and 105 RF events for PlasmaTherm RIE, 68 pump events, 80 E-gun events and 220 controller

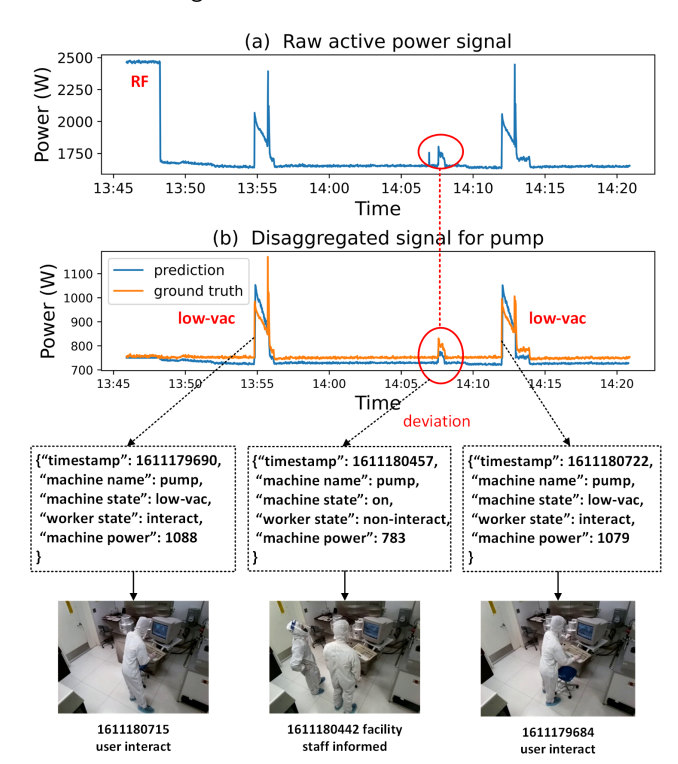


Figure 10: A combination of the second and third type of contexts is captured and illustrated. Between two pumping down (low-vac state), a small bump with actual power deviates from the average of pump on state. The corresponding WMI contexts are shown. During the anomaly occurrence, the facility staff is informed and checks the machine status.

events for E-Beam, and the two PECVD usages. We considered the precision (P) and recall (R) as the metric for the machine event classification. As shown in table 5, 6, and 7, our approach achieved better performance on all the three test cases. Particularly, the proposed method can handle the heater pulses while other methods fail to detect the pulsing mode heater as well as other events with heater pulses in a low sampling frequency. This is achieved by the segregation of the heater pulses and steady state signals. Statistical methods are widely used for abrupt steady state changes but are not effective with the heater pulses in this study as the statistical features of the signals are not stable. To extract the contextual information, it is essential to extract the signal envelope and keep the signal envelope undistorted while detecting the heater pulsing states at the same time. Because the WMI context requires reliable detection of component state transition time and the context of abnormal machine states (as the example in figure 10) requires disaggregated component-level power signals. We further tested the wavelet thresholding to remove the heater pulses as shown in figure 11. Compared with our method in figure 5(b), the wavelet thresholding as well as other regular low-pass filters can remove the pulses in some regions but highly distort the underlying signal of steady state machine components. The reason is that the pulses are not the true noise but the result of feedback control of temperature. Sometimes the heater

 Table 5

 PlasmaTherm RIE Event Classification Comparison

Method	Pu	mp	RF			
Welliou	Р	R	Р	R		
GLR[40]	0.896	0.863	0.864	0.848		
Chi square[39]	0.951	0.963	0.970	0.914		
Rehman et al.[51]	0.950	0.950	0.981	0.971		
Ours	1	1	0.99	0.99		

 Table 6

 PlasmaTherm PECVD Event Classification Comparison

Method	Pump		F	₹F	Hea	ater	Pulsing
Method	Р	R	Р	R	Р	R	Heater
GLR[40]	0.75	0.6	failed		0.526	0.909	not able
Chi square[39]	0.667	0.6	failed		failed		not able
Rehman et al.[51]	0.7	0.7	0.12	0.333	0.524	1	not able
Ours	1	1	1	1	1	1	can process

Table 7
E-Beam Event Classification Comparison

Method	Pu	mp	E-8	gun	Controller		
Welliou	Р	R	Р	R	Р	R	
GLR[40]	0.853	0.941	0.923	0.900	0.867	0.950	
Chi Square[39]	0.958	1	0.963	0.963	0.882	0.955	
Rehman et al.[51]	0.932	1	0.904	0.938	0.932	0.932	
Ours	0.986	1	1	0.975	1	0.964	

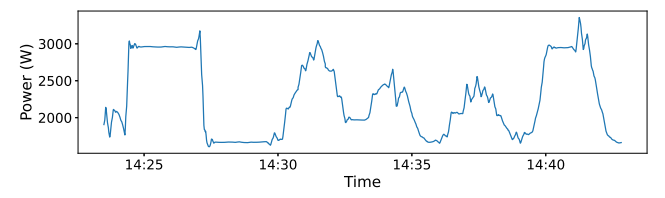


Figure 11: An example of the processed raw signal by wavelet thresholding.

stays active longer than several seconds as we can observe in figure 5, which causes that in some regions the heater pulses can have similar frequency as the base signal. In fact, the pulses have different frequency distributions with the true sensor noise (e.g., white noise), are not random, and are correlated through the feedback control. In our two-stage preprocessing method, we use the frequency analysis to identify the start and end of pulses and apply the prior knowledge of machine components to provide thresholds for removing the pulses from the base signal, instead of filtering the pulses in frequency domain.

Discussion: The FSM model generated from SOP defines the state transitions of machines and workers, and the causality between worker and machine states. This model not only helps the determination of machine component states and worker states independently, but also opens a new way of leveraging the causality to capture the contexts and further to achieve automated data labeling for ML. This paper demonstrates the effective state detection and energy disaggregation of machine components and the context capture capability by using the FSM-based SOP model. The prior knowledge of SOP and instrumentation principles

alleviates the requirement of data collection for supervised energy disaggregation and the requirement of high sampling rate of power meters. The automated data labeling can be achieved by extending this study leveraging the causality between worker actions and machine responses defined in the FSM-based SOP model. For example, recognizing worker gestures for interacting with machines is important for operation integrity. An ML model for action recognition can be trained with the collected video snaps of worker interaction moments effortlessly without any manual data collection and annotation. More importantly, each machine can have a totally different interface requiring different gestures for worker interactions. This automated data labeling method enabled by the proposed FSM-based SOP model can enhance the adaptability of ML models to dynamically adjust to different machine interfaces during deployment. The underlying concept of the causality induced automated labeling can easily be extended to various interactive activities between two objects in manufacturing. It brings a new angle of understanding manufacturing interactions. Given an assembly line as an example, materials are processed by workers or machines stage by stage with intermediate quality inspection to sense material properties. If the response time between worker/machinematerial interactions and material state transitions can be derived, the proposed concept can be applied to use the material state change to capture the worker/machine-material interaction contexts and environmental contexts to assist the product quality inspection and potential automated labeling.

Furthermore, the sequence of machine component events with anomalies are extracted with the corresponding WMI contexts. The context extracted by the proposed novel method is important in terms of several practical applications. For example, the extracted event contexts can be used to identify the integrity of worker and machine operation compared with SOP at the component level. Any deviations can lead to immediate malfunctions or unnoticed tool wear and tear accumulated to cause a serious machine breakdown in the future. The captured anomaly contexts due to the effective disaggregation of component signals can assist the development of prognosis applications. On the other hand, the disaggregated power signals with the color information from gas plasma emission can be exploited for identifying the gas type, processing duration and plasma power level, implicating a stable processing condition for manufacturing quality control.

Application Restrictions: The proposed context capture is based on the SOP-defined worker and machine state domain. There are two constraints. The first constraint is that if some unknown state occurs beyond the SOP, the system could fail in detecting the state. A perspective is to leverage the worker intelligence and predefined worker states indicating abnormal machine states and followed by unsupervised clustering methods to detect the data similarity to form a new class data for the machine and worker state detection. The second constraint is that while this study uses power signals to successfully detect machine responses of energy states, there are some cases that machines do not respond in

a way of energy consumption, such as the state of material loading. Other responsive sensors for these undetected states, such as acoustic and IR sensors, can be selected to detect the machine operation within the same cause-and-effect concept. Similarly, the corresponding worker interactions can be captured by using these additional channels of sensors. While these limitations may impede the application of the contextual sensor system, the proposed remedies shed a light on new research directions for future improvement.

6. Conclusion

In this paper, we first propose a context-centric knowledge transfer framework to address the methodology of designing a contextual SM system with the information injection from a human observer and the documented knowledge. An event-driven contextual sensor system developed upon the knowledge transfer approach is implemented and tested on multiple semiconductor fabrication machines with or without PLC and each with multiple components. The experiment results demonstrate the capability of event recognition and context awareness by using proposed processing techniques over video frame and power meter signal. We envision many potential applications as discussed in the paper could be developed.

Acknowledgement

This study is sponsored by Clean Energy Smart Manufacturing Innovation Institute (CESMII) through U.S. Department of Energy under the Award Number DE-EE0007613. The authors thank Jake Hes, Richard Chang, C. Y. Lee, and Marc Palazzo from Integrated Nanosystems Research Facility (INRF) at UCI for their technical insights of equipment and efforts to conduct several test runs for the data collection. The authors are also grateful to Dr. Richard Donovan and Dr. Michael Klopfer for their technical assistance and helpful discussions. Y. Ren wants to thank Broadcom foundation for fellowship support.

References

- [1] Y. Lu, X. Xu, L. Wang, Smart manufacturing process and system automation – a critical review of the standards and envisioned scenarios, J Manuf Syst 56 (2020) 312–325. doi:https://doi.org/ 10.1016/j.jmsy.2020.06.010.
- [2] F. Tao, Q. Qi, A. Liu, A. Kusiak, Data-driven smart manufacturing, J Manuf Syst 48 (2018) 157–169. doi:https://doi.org/10.1016/j.jmsy. 2018.01.006.
- [3] Z. Wang, M. Ritou, C. D. Cunha, B. Furet, Contextual classification for smart machining based on unsupervised machine learning by gaussian mixture model, Int J Comput Integr Manuf 33 (2020) 1042–1054. doi:10.1080/0951192X.2020.1775302.
- [4] J. Wang, S. Gao, Z. Tang, D. Tan, B. Cao, J. Fan, A context-aware recommendation system for improving manufacturing process modeling, J Intell Manuf (2021). doi:10.1007/s10845-021-01854-4.
- [5] K. Alexopoulos, K. Sipsas, E. Xanthakis, S. Makris, D. Mourtzis, An industrial internet of things based platform for context-aware information services in manufacturing, Int J Comput Integr Manuf 31 (2018) 1111–1123. doi:10.1080/0951192X.2018.1500716.

- [6] J. Leng, P. Jiang, C. Liu, C. Wang, Contextual self-organizing of manufacturing process for mass individualization: a cyber-physicalsocial system approach, Enterp Inf Syst 14 (2020) 1124–1149. doi:10.1080/17517575.2018.1470259.
- [7] E. Kaasinen, S. Aromaa, P. Heikkilä, M. Liinasuo, Empowering and engaging solutions for operator 4.0 – acceptance and foreseen impacts by factory workers, in: F. Ameri, K. E. Stecke, G. von Cieminski, D. Kiritsis (Eds.), Advances in Production Management Systems. Production Management for the Factory of the Future, Springer International Publishing, Cham, 2019, pp. 615–623.
- [8] D. Şahinel, C. Akpolat, O. C. Görür, F. Sivrikaya, S. Albayrak, Human modeling and interaction in cyber-physical systems: A reference framework, J Manuf Syst 59 (2021) 367–385. doi:https://doi.org/10. 1016/j.jmsy.2021.03.002.
- [9] Q. Xiong, J. Zhang, P. Wang, D. Liu, R. X. Gao, Transferable two-stream convolutional neural network for human action recognition, J Manuf Syst 56 (2020) 605–614. doi:https://doi.org/10.1016/j.jmsy.2020.04.007.
- [10] N. Azouz, H. Pierreval, Adaptive smart card-based pull control systems in context-aware manufacturing systems: Training a neural network through multi-objective simulation optimization, Appl Soft Comput 75 (2019) 46–57. doi:https://doi.org/10.1016/j.asoc.2018.10.051.
- [11] A. Al-Shdifat, C. Emmanouilidis, Development of a context-aware framework for the integration of internet of things and cloud computing for remote monitoring services, Procedia Manuf 16 (2018) 31–38. doi:https://doi.org/10.1016/j.promfg.2018.10.155.
- [12] P. Wang, H. Liu, L. Wang, R. X. Gao, Deep learning-based human motion recognition for predictive context-aware human-robot collaboration, CIRP Annals 67 (2018) 17–20. doi:https://doi.org/10. 1016/j.cirp.2018.04.066.
- [13] J. Wan, S. Tang, Q. Hua, D. Li, C. Liu, J. Lloret, Context-aware cloud robotics for material handling in cognitive industrial internet of things, IEEE Internet Things J 5 (2018) 2272–2281. doi:10.1109/JIOT.2017. 2728722
- [14] K. Alexopoulos, S. Makris, V. Xanthakis, K. Sipsas, G. Chryssolouris, A concept for context-aware computing in manufacturing: the white goods case, Int J Comput Integr Manuf 29 (2016) 839–849. doi:10. 1080/0951192X.2015.1130257.
- [15] L. Horváth, Contextual knowledge content driving for model of cyber physical system, in: 2018 15th International Conference on Control, Automation, Robotics and Vision (ICARCV), 2018, pp. 1845–1850. doi:10.1109/ICARCV.2018.8581371.
- [16] C. Emmanouilidis, P. Pistofidis, A. Fournaris, M. Bevilacqua, I. Durazo-Cardenas, P. N. Botsaris, V. Katsouros, C. Koulamas, A. G. Starr, Context-based and human-centred information fusion in diagnostics, IFAC-PapersOnLine 49 (2016) 220–225. doi:https://doi.org/10.1016/j.ifacol.2016.11.038.
- [17] Z. Wang, M. Ritou, C. D. Cunha, B. Furet, Contextual classification for smart machining based on unsupervised machine learning by gaussian mixture model, Int J Comput Integr Manuf 33 (2020) 1042–1054. doi:10.1080/0951192X.2020.1775302.
- [18] Y. Guo, Y. Sun, K. Wu, Research and development of monitoring system and data monitoring system and data acquisition of cnc machine tool in intelligent manufacturing, Int J Adv Robot Syst 17 (2020). doi:10.1177/1729881419898017.
- [19] K.-J. Wang, Y.-H. Lee, S. Angelica, Digital twin design for real-time monitoring – a case study of die cutting machine, Int J Prod Res 0 (2020) 1–15. doi:10.1080/00207543.2020.1817999.
- [20] A. M. Deshpande, A. K. Telikicherla, V. Jakkali, D. A. Wickelhaus, M. Kumar, S. Anand, Computer vision toolkit for non-invasive monitoring of factory floor artifacts, Procedia Manuf 48 (2020) 1020– 1028. doi:https://doi.org/10.1016/j.promfg.2020.05.141.
- [21] N. Panten, E. Abele, S. Schweig, A power disaggregation approach for fine-grained machine energy monitoring by system identification, Procedia CIRP 48 (2016) 325 – 330. doi:https://doi.org/10.1016/j. procir.2016.03.025.
- [22] C.-Y. Cheng, A novel approach of information visualization for machine operation states in industrial 4.0, Comput Ind Eng 125 (2018)

- 563 573. doi:https://doi.org/10.1016/j.cie.2018.05.024.
- [23] J. Sossenheimer, T. Weber, D. Flum, N. Panten, E. Abele, T. Fuertjes, Non-intrusive Load Monitoring on Component Level of a Machine Tool Using a Kalman Filter-Based Disaggregation Approach, Springer International Publishing, Cham, 2019, pp. 155–165. doi:10.1007/ 978-3-030-02203-7_9.
- [24] J. Sossenheimer, O. Vetter, E. Abele, M. Weigold, Hybrid virtual energy metering points – a low-cost energy monitoring approach for production systems based on offline trained prediction models, Procedia CIRP 93 (2020) 1269–1274. doi:https://doi.org/10.1016/j. procir.2020.04.128.
- [25] C. Qian, Y. Zhang, C. Jiang, S. Pan, Y. Rong, A real-time data-driven collaborative mechanism in fixed-position assembly systems for smart manufacturing, Robot Comput Integr Manuf 61 (2020) 101841. doi:https://doi.org/10.1016/j.rcim.2019.101841.
- [26] L. Hu, H. Zheng, L. Shu, S. Jia, W. Cai, K. Xu, An investigation into the method of energy monitoring and reduction for machining systems, J Manuf Syst 57 (2020) 390–399. doi:https://doi.org/10.1016/j.jmsy. 2020.10.012.
- [27] B. Lu, V. C. Gungor, Online and remote motor energy monitoring and fault diagnostics using wireless sensor networks, IEEE Trans Ind Electron 56 (2009) 4651–4659. doi:10.1109/TIE.2009.2028349.
- [28] R. Y. Zhong, L. Wang, X. Xu, An iot-enabled real-time machine status monitoring approach for cloud manufacturing, Procedia CIRP 63 (2017) 709–714. doi:https://doi.org/10.1016/j.procir.2017.03.349.
- [29] B. Edrington, B. Zhao, A. Hansel, M. Mori, M. Fujishima, Machine monitoring system based on mtconnect technology, Procedia CIRP 22 (2014) 92–97. doi:https://doi.org/10.1016/j.procir.2014.07.148.
- [30] R. Drake, M. Yildirim, J. Twomey, L. Whitman, J. Sheikh-Ahmad, P. Lodhia, Data collection framework on energy consumption in manufacturing, Proceedings of 2006 Institute of Industrial Engineering Research Conference (2006).
- [31] Y. S. Tan, Y. T. Ng, J. S. C. Low, Internet-of-things enabled real-time monitoring of energy efficiency on manufacturing shop floors, Procedia CIRP 61 (2017) 376–381. doi:https://doi.org/10.1016/j.procir.2016.11.242.
- [32] S. Han, N. Mannan, D. C. Stein, K. R. Pattipati, G. M. Bollas, Classification and regression models of audio and vibration signals for machine state monitoring in precision machining systems, J Manuf Syst 61 (2021) 45–53. doi:https://doi.org/10.1016/j.jmsy.2021.08.004.
- [33] S. S. Hosseini, K. Agbossou, S. Kelouwani, A. Cardenas, Non-intrusive load monitoring through home energy management systems: A comprehensive review, Renew Sust Energ Rev 79 (2017) 1266–1274. doi:https://doi.org/10.1016/j.rser.2017.05.096.
- [34] L. Hattam, D. V. Greetham, Energy disaggregation for smes using recurrence quantification analysis, in: Proceedings of the Ninth International Conference on Future Energy Systems, 2018, p. 610–617. doi:https://doi.org/10.1145/3208903.3210280.
- [35] P. B. M. Martins, J. G. R. C. Gomes, V. B. Nascimento, A. R. de Freitas, Application of a deep learning generative model to load disaggregation for industrial machinery power consumption monitoring, in: 2018 IEEE International Conference on Communications, Control, and Computing Technologies for Smart Grids (SmartGridComm), 2018, pp. 1–6. doi:10.1109/SmartGridComm.2018.8587415.
- [36] A. Zoha, A. Gluhak, M. A. Imran, S. Rajasegarar, Non-intrusive load monitoring approaches for disaggregated energy sensing: A survey, Sensors 12 (2012) 16838–16866. doi:10.3390/s121216838.
- [37] W. Wichakool, Z. Remscrim, U. A. Orji, S. B. Leeb, Smart metering of variable power loads, IEEE Trans Smart Grid 6 (2015) 189–198. doi:10.1109/TSG.2014.2352648.
- [38] P. A. Lindahl, M. T. Ali, P. Armstrong, A. Aboulian, J. Donnal, L. Norford, S. B. Leeb, Nonintrusive load monitoring of variable speed drive cooling systems, IEEE Access 8 (2020) 211451–211463. doi:10.1109/ACCESS.2020.3039408.
- [39] Y. Jin, E. Tebekaemi, M. Berges, L. Soibelman, Robust adaptive event detection in non-intrusive load monitoring for energy aware smart facilities, in: 2011 IEEE International Conference on Acoustics, Speech and Signal Processing (ICASSP), 2011, pp. 4340–4343. doi:10.

- 1109/ICASSP.2011.5947314.
- [40] K. D. Anderson, M. E. Bergés, A. Ocneanu, D. Benitez, J. M. Moura, Event detection for non intrusive load monitoring, in: IECON 2012 -38th Annual Conference on IEEE Industrial Electronics Society, 2012, pp. 3312–3317. doi:10.1109/IECON.2012.6389367.
- [41] R. Yadav, A. K. Pradhan, I. Kamwa, Real-time multiple event detection and classification in power system using signal energy transformations, IEEE Trans Industr Inform 15 (2019) 1521–1531. doi:10.1109/TII.2018.2855428.
- [42] A. U. Rehman, T. T. Lie, B. Vallès, S. R. Tito, Event-detection algorithms for low sampling nonintrusive load monitoring systems based on low complexity statistical features, IEEE Trans Instrum Meas 69 (2020) 751–759. doi:10.1109/TIM.2019.2904351.
- [43] Álvaro Segura, H. V. Diez, I. Barandiaran, A. Arbelaiz, H. Álvarez, B. Simões, J. Posada, A. García-Alonso, R. Ugarte, Visual computing technologies to support the operator 4.0, Comput Ind Eng 139 (2020) 105550. doi:https://doi.org/10.1016/j.cie.2018.11.060.
- [44] I. Zolotová, P. Papcun, E. Kajáti, M. Miškuf, J. Mocnej, Smart and cognitive solutions for operator 4.0: Laboratory h-cpps case studies, Comput Ind Eng 139 (2020) 105471. doi:https://doi.org/10.1016/j. cie.2018.10.032.
- [45] E. Kaasinen, F. Schmalfuß, C. Özturk, S. Aromaa, M. Boubekeur, J. Heilala, P. Heikkilä, T. Kuula, M. Liinasuo, S. Mach, R. Mehta, E. Petäjä, T. Walter, Empowering and engaging industrial workers with operator 4.0 solutions, Comput Ind Eng 139 (2020) 105678. doi:https://doi.org/10.1016/j.cie.2019.01.052.
- [46] C. Cimini, F. Pirola, R. Pinto, S. Cavalieri, A human-in-the-loop manufacturing control architecture for the next generation of production systems, J Manuf Syst 54 (2020) 258–271. URL: https://www.sciencedirect.com/science/article/pii/S0278612520300029. doi:https://doi.org/10.1016/j.jmsy.2020.01.002.
- [47] T. Wuest, C. Irgens, K.-D. Thoben, An approach to monitoring quality in manufacturing using supervised machine learning on product state data, J Intell Manuf 25 (2014) 1167–1180. doi:10.1007/ s10845-013-0761-y.
- [48] H.-C. Lee, Review of inductively coupled plasmas: Nano-applications and bistable hysteresis physics, Appl Phys Rev 5 (2018) 011108. doi:10.1063/1.5012001.
- [49] A. Merkhouf, M. I. Boulos, Integrated model for the radio frequency induction plasma torch and power supply system, Plasma Sources Sci Technol 7 (1998) 599–606. doi:10.1088/0963-0252/7/4/017.
- [50] N. Batra, R. Kukunuri, A. Pandey, R. Malakar, R. Kumar, O. Krystalakos, M. Zhong, P. Meira, O. Parson, Towards reproducible state-of-the-art energy disaggregation, in: Proceedings of the 6th ACM International Conference on Systems for Energy-Efficient Buildings, Cities, and Transportation, 2019, p. 193–202. doi:https://doi.org/10.1145/3360322.3360844.
- [51] A. U. Rehman, S. Rahman Tito, T. T. Lie, P. Nieuwoudt, N. Pandey, D. Ahmed, B. Vallès, Non-intrusive load monitoring: A computationally efficient hybrid event detection algorithm, in: 2020 IEEE International Conference on Power and Energy (PECon), 2020, pp. 304–308. doi:10.1109/PECon48942.2020.9314442.